Journal of Magnetism and Magnetic Materials 392 (2015) 79–82

Contents lists available at ScienceDirect

Journal of Magnetism and Magnetic Materials

journal homepage: www.elsevier.com/locate/jmmm

Temperature dependence of the perpendicular magnetic anisotropy in Ta/Co_2FeAl/MgO structures probed by Anomalous Hall Effect

M.S. Gabor [a,*], T. Petrisor Jr.[a], O. Pop [b], S. Colis [c], C. Tiusan [d,e]

[a] Center for Superconductivity, Spintronics and Surface Science, Physics and Chemistry Department, Technical University of Cluj-Napoca, Str. Memorandumului No. 28, RO-400114 Cluj-Napoca, Romania
[b] Applied Electronics Department, Faculty of Electronics, Telecommunications and Information Technology, Technical University of Cluj-Napoca, Str. Memorandumului No. 28, RO-400114 Cluj-Napoca, Romania
[c] Institut de Physique et Chimie des Materiaux de Strasbourg (IPCMS), UMR 7504 UDS-CNRS and Université de Strasbourg (UDS-ECPM), 23 rue du Loess, BP43, F-67034 Strasbourg Cedex 2, France
[d] Center for Superconductivity, Spintronics and Surface Science, Physics and Chemistry Department, Technical University of Cluj-Napoca, Str. Memorandumului No. 28, RO-400114 Cluj-Napoca, Romania
[e] Institut Jean Lamour, CNRS, Université de Lorraine, F-54506 Vandoeuvre, France

ARTICLE INFO

Article history:
Received 14 February 2015
Received in revised form
26 April 2015
Accepted 8 May 2015
Available online 9 May 2015

ABSTRACT

We report a detailed study of the temperature dependence of the magnetic anisotropy in Ta/Co_2FeAl/MgO structures by means of Anomalous Hall Effect measurements. The volume magnetic anisotropy, although negligible at room temperature, shows a non-negligible value at low temperatures and favors an in-plane easy magnetization axis. The surface magnetic anisotropy, which promotes the perpendicular magnetic easy axis, shows an increase from 0.76 ± 0.05 erg/cm^2 at 300 K, up to 1.08 ± 0.04 erg/cm^2 at 5 K, attributed to the evolution of the Co_2FeAl layer saturation magnetization with temperature.

1. Introduction

Ultrathin magnetic films are attracting considerable research interest from both fundamental and applications points of view. In particular, ferromagnetic (FM) films showing perpendicular magnetic anisotropy (PMA) are of special importance due to their use for perpendicular magnetic recording technology, including bit-patterned media, racetrack and spin transfer torque magnetic random access memories (STT-MRAM) [1–3]. The conventional PMA systems comprise the $L1_0$ ordered alloys (FePt and CoPt), Co-based multilayers (Co/Pd and Co/Pt) and rare-earth and transition metal alloys [4–10]. An important advantage of spintronic devices with FM electrodes showing PMA is that, due to the absence of the demagnetization term, they allow reducing the spin transfer torque (STT) switching current density (J_{c0}) [11,12], which is also dependent on the Gilbert damping constant α and on the spin polarization [13]. An alternative route to obtain PMA is by exploiting the FM transition metal/oxide interfacial magnetic anisotropy [14–16], commonly attributed, from first principles calculations, to the hybridization of the O 2*p* and Co or Fe 3*d* orbitals [17–19]. This allows to avoid the use of large spin–orbit coupling (SOC) elements like Pd or Pt which have a detrimental effect on both Gilbert damping and spin polarization of the FM material. Since it was shown to provide giant tunneling magnetoresistance (GTMR) in MgO based magnetic tunnel junctions (MTJs) [20–25], to possess a low Gilbert damping [26,27] and to provide PMA in Pt/CFA/MgO, Cr/CFA/MgO, Ta/CFA/MgO and Ru/CFA/MgO structures [28–31], the full Heulser alloy Co_2FeAl (CFA) proves itself as an important candidate to be used in STT-MTJs based spintronic devices.

For a ferromagnetic thin film the transverse Hall resistivity (ρ_{xy}) was found [32] to follow the empirical relation: $\rho_{xy} = R_0 H + R_S 4\pi M_z$, where R_0 and R_S are the ordinary and anomalous Hall constants, H is the applied perpendicular magnetic field, while M_z is the magnetization along the perpendicular to the plane direction. The normal Hall contribution is a consequence of the Lorentz force acting on the conduction electrons and it manifests itself as a linear dependence of ρ_{xy} on the field H, discernible at relative high fields, where the magnetization is saturated. Usually, the normal Hall component is much smaller than the anomalous one and as a result, below saturation, the Hall resistivity is essentially proportional with the out-of-plane component of the magnetization. Therefore, the Anomalous Hall Effect (AHE), as a manifestation of magnetism on electronic transport, is a useful tool for studying the magnetic properties of ultrathin

* Corresponding author.
E-mail addresses: Mihai.Gabor@phys.utcluj.ro (M.S. Gabor), Coriolan.Tiusan@phys.utcluj.ro (C. Tiusan).

http://dx.doi.org/10.1016/j.jmmm.2015.05.013
0304-8853/

magnetic films and multilayers. In this paper, we use AHE in order to study the temperature dependence of the perpendicular magnetic anisotropy in Ta/CFA/MgO multilayers.

2. Experimental

The Si/SiO_x/Ta(4 nm)/CFA(1.1-4.5 nm)/MgO(1.3 nm)/Ta(1.2 nm) multilayer stacks were elaborated using magnetron sputtering. Details about the growth and crystal structure of the stacks can be found in our previous work [30]. After deposition, the multilayers were *ex situ* annealed for one hour at 200 °C in vacuum. The saturation magnetization of the films was studied using Superconducting Quantum Interference Device (SQUID) magnetometry. For the electronic transport measurements the samples were patterned by UV lithography in the form of Hall bars [inset of Fig. 1(a)]. Hall experiments were performed using a standard DC technique in a temperature range between 5 and 300 K and in magnetic fields up to 7 T.

3. Results and discussions

Fig. 1 shows representative Hall loops for CFA films with nominal thicknesses of 1.1 and 2.4 nm measured at 5 and 300 K. In the case of the 2.4 nm thick film, the measurements indicate an in-plane magnetic anisotropy and the coherent rotation of the magnetization towards the out-of-plane direction as the magnetic field is increased. In the case of the 1.1 nm thick film the Hall loops show a square shape with full remanence (Mr/Ms=1) and with a coercive field that increases as the temperature is decreased. This is expected as a consequence of the reduction of the thermally activated magnetization reversal processes [inset of Fig. 1(b)]. The square shape of the loops indicates the presence of perpendicular magnetic anisotropy for the 1.1 nm thick CFA film in the whole temperature range.

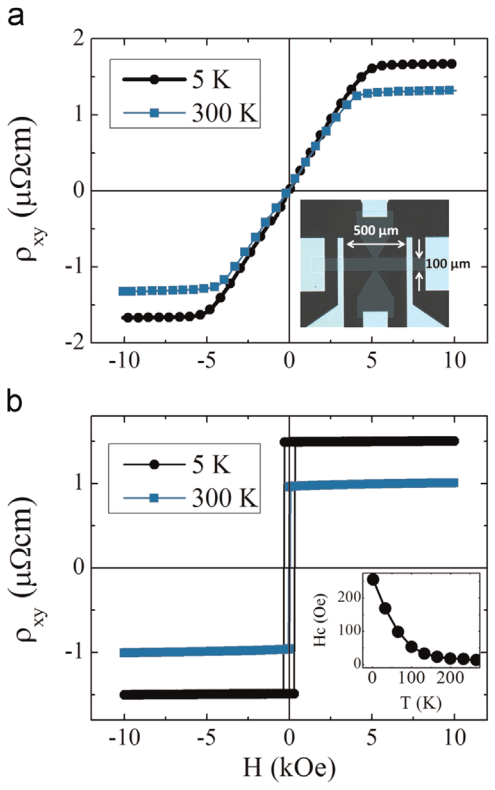

Fig. 1. Transverse Hall resistivity as a function of the perpendicular magnetic field for the (a) 2.4 nm and (b) 1.1 nm thick CFA films, measured at 5 and 300 K. The inset of (a) shows an optical microscopy image of a Hall patterned element. The inset of (b) shows the temperature dependence of the coercive field of the Hall loops measured for the 1.1 nm thick CFA film.

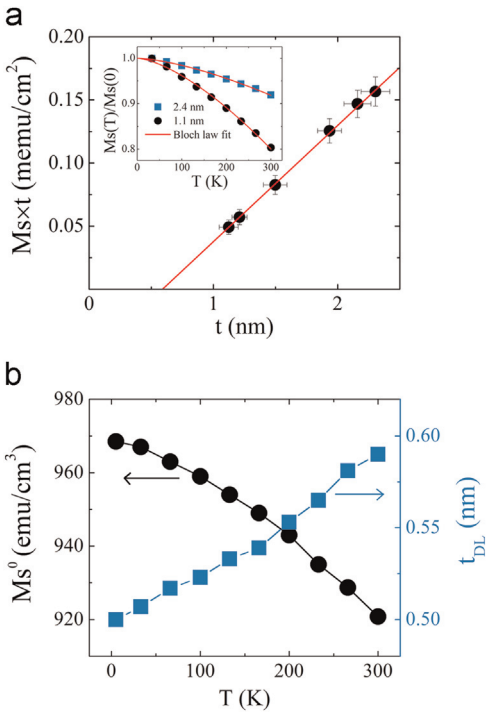

Fig. 2. (a) The sheet saturation magnetization ($M_S \times t$) as a function of CFA nominal thickness (t) measured at 300 K. The inset shows the temperature dependence of the normalized saturation magnetization for the 1.1 and the 2.4 nm thick CFA films. (b) The temperature dependence of the *magnetic dead layer* thickness and of the mean saturation magnetization.

In order to characterize the magnetic properties of our films we performed SQUID measurements on samples with different CFA thicknesses. Fig. 2 shows a plot of the sheet saturation magnetization ($M_S \times t$) as a function of CFA nominal thickness (t), measured at 300 K. In this representation, the intercept of the linear fit with the horizontal axis gives the extent of the *magnetic dead layer* (MDL), while the slope gives the mean saturation magnetization (M_S^0) of the CFA films. Most likely, the MDL is a result of the interdiffusion at the Ta–CFA interface. The thickness of the MDL is around 0.6 nm at RT and shows a slight decrease down to 0.5 nm as the temperature is decreased down to 4 K [Fig. 2(b)]. Furthermore, the as-determined mean saturation magnetization shows an increase from around 920 emu/cm^3 at RT, up to around 970 emu/cm^3 at 5 K. The inset of Fig. 2(a) shows the temperature dependence of the normalized saturation magnetization, determined from the SQUID hysteresis loops, for the 1.1 and the 2.4 nm thick CFA films, respectively. Between 5 and 300 K the data are well fitted by the three dimensional Bloch spin-wave law $M_S(T) = M_S(0)(1 - bT^{3/2})$, where $M_S(0)$ is the spontaneous magnetization at 0 K and b is the spin-wave parameter [33]. The normalized spontaneous magnetization $[M_S(T)/M_S(0)]$ of the 1.1 nm thick CFA film shows a stronger temperature dependence as compared to the 2.4 nm thick one. This is an indication of the reduced Curie temperature of the 1.1 nm thick film relative to the 2.4 nm one. This is expected, having in view the reduced average coordination number of the thinner film relative to the thicker one, due to the relative increase of the surface spins density [34,33].

The different magnetic anisotropy contributions were quantified from the Hall effect measurements in the case of the in-plane magnetized films, and planar Hall measurements in the case of the out-of-plane magnetized ones. The anisotropy constants were

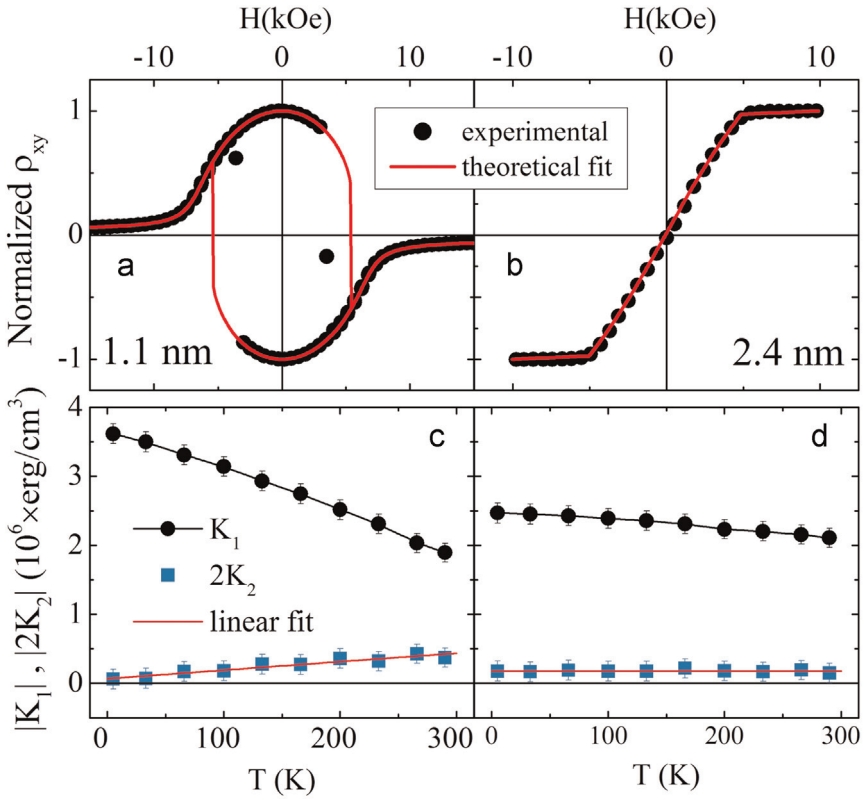

Fig. 3. Measured and simulated planar Hall (a) and Hall (b) effect curves for the 1.1 and 2.4 nm thick CFA films. (c) Temperature dependence of the second (K_1) and fourth (K_2) order anisotropy constants for the 1.1 (c) and 2.4 nm (d) thick CFA films.

extracted by fitting the measured data within the Stoner–Wohlfarth (S–W) coherent rotation model [35], using the following energy expression: $E = K_1 m_z^2 + K_2 m_z^4 - \mathbf{MH}$, where K_1 and K_2 are the second and the fourth order uniaxial anisotropy constants, m_z is the direction cosine of the magnetization **M** and the last term represents the Zeeman energy. We have simulated numerically the Hall and planar Hall curves using as parameters the K_1 and K_2 constants. Using a least square algorithm, the values of K_1 and K_2 were optimized until the best fit to the experimental data was obtained. Fig. 3 (a) and (b) shows the result of such calculations compared to the experimental data measured at 5 K for the 1.1 nm (planar Hall) and 2.4 nm (Hall) thick CFA films. A very good agreement between the experimental data and the simulations can be observed, except for the switching region. Since the S–W model does not accommodate irreversible effects such as domain walls nucleation and propagation, the switching fields are overestimated. However, this does not affect the correctness of the K_1 and K_2 evaluation. Fig. 3 (c) and (d) shows the as-determined values of the K_1 and K_2 as a function of temperature for the 1.1 nm and 2.4 nm thick films. It can be easily noticed that K_1 shows a stronger temperature dependence for the 1.1 nm thick film relative to the 2.4 nm thick one. This can be understood if the interface anisotropy term is considered and will be discussed in the next paragraph. Moreover, the value of K_2 corresponding to the 1.1 nm CFA film, although negligibly small at 5 K, shows a monotonous increase with temperature up to a value of $2K_2 = (0.38 \pm 0.14) \times 10^6$ erg/cm^3 at 300 K. At this temperature the value of K_1 is around $(1.89 \pm 0.13) \times 10^6$ erg/cm^3. In the case of the 2.4 nm thick film, the K_2 shows negligibly small values in the whole temperature range with no obvious temperature dependence. It is known [34] that for a thin film for which the interface anisotropy favors a perpendicular magnetization alignment, due to the competition with shape anisotropy, which favors an in-plane magnetization configuration, a *vertical non-collinear* magnetization orientation can develop. In this configuration, the magnetization is homogeneously aligned in each atomic layer but changes direction, in the different atomic layers, when going form one interface towards the other. From an energetic point of view this is equivalent with the presence of higher anisotropy term like the fourth order (K_2). When increasing the temperature, due to thermal fluctuations, the *noncollinearity* is augmented. This leads to an increase of K_2, as the one observed in the present study.

To quantify the PMA we define the effective anisotropy constant as $K_{eff} = K_1 + 2K_2$. In our model, K_{eff} is positive for perpendicular easy axis and negative in the case of in plane magnetic easy axis. The K_{eff} can be described by the phenomenological relation [33]: $K_{\text{eff}} \times t_{\text{eff}} = \left[K_v - 2\pi\left(M_S^0\right)^2\right] \times t_{\text{eff}} + K_S$, where K_v describes the bulk magnetic anisotropy, $2\pi\left(M_S^0\right)^2$ the shape magnetic anisotropy and K_S the surface (interface) magnetic anisotropy. By fitting the t_{eff} (CFA layer effective thickness) dependence of the product $K_{eff} \times t_{eff}$ the different anisotropy contributions can be evaluated. Fig. 4(a) shows the result of such an analysis for the measurements performed at 300 K. In Fig. 4(b) the temperature dependence of the as-determined surface and bulk magnetic anisotropy contributions are illustrated. One can observe that the volume anisotropy is within the limit of the error bars negligible at RT, and that its value becomes non-negligible at low temperatures. The volume anisotropy is expected to result from magnetocrystalline and/or magnetoelastic contributions. Given the polycrystalline nature of the CFA films grown on Ta [30] it is reasonable to assume that K_v is not of magnetocrystalline origin. Therefore, a strain related contribution via the magnetoelastic coupling has to be considered. Although, strains can be induced by various mechanisms, the ones that are most probable in our case are the intrinsic strains developed during film growth and/or the thermal strains

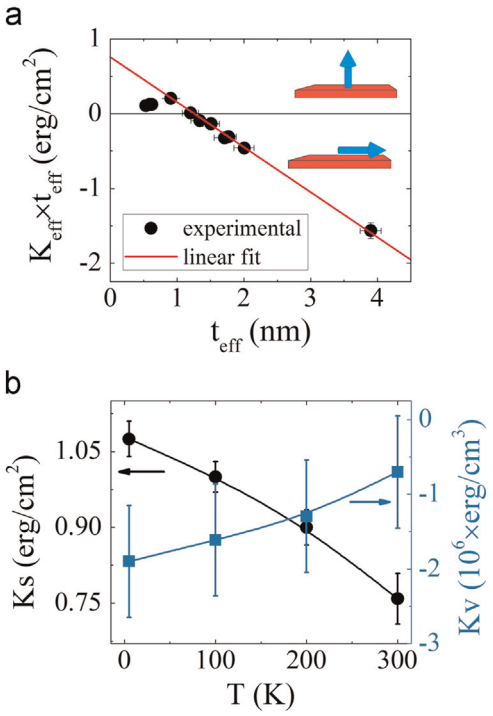

Fig. 4. (a) Effective anisotropy times effective thickness vs effective thickness at 300 K. (b) K_s and K_v dependence on temperature. The lines serve only as visual guides.

associated with differences in the thermal expansion coefficients of the different layers and substrate. Indeed, in a recent paper it was demonstrated that CFA magnetoelastic coefficients show a strong temperature variation [36]. Therefore, even if at RT the contribution to the magnetic anisotropy by intrinsic strains might be negligible, at low temperatures, a strong increase of the magnetoelastic coefficients might induce a non-negligible contribution via the magnetoelastic coupling. Similar to the volume anisotropy, K_s shows an important increase when decreasing temperature from 0.76 ± 0.05 erg/cm^2 at 300 K, up to 1.08 ± 0.04 erg/cm^2 at 5 K. Contrary to K_v the sign of K_s is positive which is a confirmation that K_s alone is responsible for the PMA. Although we cannot exclude the variation of the surface electronic structure with temperature, we attribute the decrease of K_s with temperature mainly to the decrease of the saturation magnetization with temperature [inset of Fig. 2(a)]. Indeed, it is already known that the increase of the thermal agitation results in a decrease of the effectiveness of the anisotropy to maintain a certain direction of the magnetization. This is equivalent to a reduction of the anisotropy constant with temperature [37], as observed in the case of our films.

4. Conclusions

In summary, we have performed a detailed study on the temperature dependence of the magnetic anisotropy in Ta/CFA/MgO structures. Our analysis has been mainly based on transport experiments in variable field and temperature using the Anomalous Hall Effect. For this purpose, the multilayer thin film samples have been patterned in strip-lines structures with Hall geometry via UV lithography and ion beam etching. The results of our studies point out an important increase of surface magnetic anisotropy from 0.76 ± 0.05 erg/cm^2 at 300 K up to 1.08 ± 0.04 erg/cm^2 at 5 K. Corroborated with standard SQUID magnetometry analysis, we have attributed this behavior to the evolution of the saturation magnetization with temperature. Moreover, the bulk magnetic anisotropy, although negligible at RT, shows a non-negligible value at low temperatures.

Acknowledgments

This work has been partially supported by the Exploratory Research Project SPINTAIL: PN-II-ID-PCE-2012-4-0315, No. 23/29.08.2013, by the project SPINTRONIC: POS CCE ID. 574, code SMIS-CSNR 12467 and by TUCN-MADSPIN Research Project.

References

[1] C. Ross, Annu. Rev. Mater. Res. 31 (2001) 203.
[2] T. Kawahara, K. Ito, R. Takemura, H. Ohno, Microelectron. Reliab. 52 (2012) 613.
[3] S.S.P. Parkin, M. Hayashi, L. Thomas, Science 320 (2008) 190.
[4] N. Nishimura, T. Hirai, A. Koganei, T. Ikeda, K. Okano, Y. Sekiguchi, Y. Osada, J. Appl. Phys. 91 (2002) 5246.
[5] H. Ohmori, T. Hatori, S. Nakagawa, J. Appl. Phys. 103 (2008) 07A911.
[6] G. Kim, Y. Sakuraba, M. Oogane, Y. Ando, T. Miyazaki, Appl. Phys. Lett. 92 (2008) 172502.
[7] K. Yakushiji, T. Saruya, H. Kubota, A. Fukushima, T. Nagahama, S. Yuasa, K. Ando, Appl. Phys. Lett. 97 (2010) 232508.
[8] J.H. Park, C. Park, T. Jeong, M.T. Moneck, N.T. Nufer, J.G. Zhu, J. Appl. Phys. 103 (2008) 07A917.
[9] B. Carvello, C. Ducruet, B. Rodmacq, S. Auffret, E. Gautier, G. Gaudin, B. Dieny, Appl. Phys. Lett. 92 (2008) 102508.
[10] A. Barman, S. Wang, O. Hellwig, A. Berger, E.E. Fullerton, H. Schmidt, J. Appl. Phys. 101 (2007) 09D102.
[11] S. Yakata, H. Kubota, Y. Suzuki, K. Yakushiji, A. Fukushima, S. Yuasa, K. Ando, J. Appl. Phys. 105 (2009) 07D131.
[12] S. Mangin, D. Ravelosona, J.A. Katine, M.J. Carey, B.D. Terris, E.E. Fullerton, Nat. Mater. 5 (2006) 210.
[13] D. Ralph, M. Stiles, J. Magn. Magn. Mater. 320 (2008) 1190.
[14] S. Ikeda, K. Miura, H. Yamamoto, K. Mizunuma, H.D. Gan, M. Endo, S. Kanai, J. Hayakawa, F. Matsukura, H. Ohno, Nat. Mater. 9 (2010) 721.
[15] S. Monso, B. Rodmacq, S. Auffret, G. Casali, F. Fettar, B. Gilles, B. Dieny, P. Boyer, Appl. Phys. Lett. 80 (2002) 4157.
[16] L.E. Nistor, B. Rodmacq, S. Auffret, B. Dieny, Appl. Phys. Lett. 94 (2009) 012512.
[17] H.X. Yang, M. Chshiev, B. Dieny, J.H. Lee, A. Manchon, K.H. Shin, Phys. Rev. B 84 (2011) 054401.
[18] A. Hallal, H.X. Yang, B. Dieny, M. Chshiev, Phys. Rev. B 88 (2013) 184423.
[19] R. Vadapoo, A. Hallal, M. Chshiev, ArXiv eprints (2014), arXiv:1404.5646 [cond-mat.mtrl-sci].
[20] W. Wang, H. Sukegawa, R. Shan, S. Mitani, K. Inomata, Appl. Phys. Lett. 95 (2009) 182502.
[21] W. Wang, E. Liu, M. Kodzuka, H. Sukegawa, M. Wojcik, E. Jedryka, G.H. Wu, K. Inomata, S. Mitani, K. Hono, Phys. Rev. B 81 (2010) 140402.
[22] W. Wang, H. Sukegawa, K. Inomata, Phys. Rev. B 82 (2010) 092402.
[23] Z. Wen, H. Sukegawa, S. Mitani, K. Inomata, Appl. Phys. Lett. 98 (2011) 192505.
[24] Z. Wen, H. Sukegawa, S. Kasai, K. Inomata, S. Mitani, Phys. Rev. Appl. 2 (2014) 024009.
[25] Z. Wen, H. Sukegawa, S. Kasai, M. Hayashi, S. Mitani, K. Inomata, Appl. Phys. Express 5 (2012) 063003.
[26] S. Mizukami, D. Watanabe, M. Oogane, Y. Ando, Y. Miura, M. Shirai, T. Miyazaki, J. Appl. Phys. 105 (2009) 07D306.
[27] M. Belmeguenai, H. Tuzcuoglu, M.S. Gabor, T. Petrisor, C. Tiusan, D. Berling, F. Zighem, T. Chauveau, S.M. Chérif, P. Moch, Phys. Rev. B 87 (2013) 184431.
[28] X. Li, S. Yin, Y. Liu, D. Zhang, X. Xu, J. Miao, Y. Jiang, Appl. Phys. Express 4 (2011) 043006.
[29] Z. Wen, H. Sukegawa, S. Mitani, K. Inomata, Appl. Phys. Lett. 98 (2011) 242507.
[30] M.S. Gabor, T. Petrisor, C. Tiusan, T. Petrisor, J. Appl. Phys. 114 (2013) 063905.
[31] Z. Wen, H. Sukegawa, T. Furubayashi, J. Koo, K. Inomata, S. Mitani, J.P. Hadorn, T. Ohkubo, K. Hono, Adv. Mater. 26 (2014) 6483.
[32] N. Nagaosa, J. Sinova, S. Onoda, A.H. MacDonald, N.P. Ong, Rev. Mod. Phys. 82 (2010) 1539.
[33] C.A.F. Vaz, J.A.C. Bland, G. Lauhoff, Rep. Prog. Phys. 71 (2008) 056501.
[34] P. Jensen, K. Bennemann, Surf. Sci. Rep. 61 (2006) 129.
[35] E.C. Stoner, E.P. Wohlfarth, Philos. Trans. R. Soc. Lond. Ser. A, Math. Phys. Sci. 240 (1948) 599.
[36] H.C. Yuan, S.H. Nie, T.P. Ma, Z. Zhang, Z. Zheng, Z.H. Chen, Y.Z. Wu, J.H. Zhao, H.B. Zhao, L.Y. Chen, Appl. Phys. Lett. 105 (2014) 072413.
[37] H. Callen, E. Callen, J. Phys. Chem. Solids 27 (1966) 1271.